J. Fluid Mech. (1972), *vol.* 51, *part* 1, *pp.* 15–32
Printed in Great Britain

The structure and stability of vortex rings

By T. MAXWORTHY

Departments of Aerospace and Mechanical Engineering, University of Southern California, Los Angeles, California, U.S.A.

(Received 24 August 1970 and in revised form 19 July 1971)

A series of observations on experimentally produced vortex rings is described. The flow field, ring velocity and growth rate were observed using dye and hydrogen-bubble techniques. It was found that stable rings are formed and grow in such a way that most of their vorticity is distributed throughout a fluid volume which is larger than and moving with the visible dye core.

As the vorticity diffuses out of this moving body of fluid into the outer irrotational fluid, it has two effects. It causes some of the fluid, with newly acquired vorticity, to be entrained into the interior of the bubble, while the rest is left behind and accounts for the appearance of ring vorticity in a wake. It was found that the velocity of translation U of these stable rings varies as t^{-1}, at high Reynolds number, where t is the time measured from the start of the motion at a virtual origin at downstream infinity. A simple theoretical model is presented which explains all of these features of the observed stable flow. Rings of even higher Reynolds number become unstable and shed significantly more vorticity into the wake. Under some circumstances a new more stable vortex emerges from this shedding process and continues with less vorticity than before. Eventually, the ring motion ceases as all of its vorticity is deposited into the wake and is spread by viscous diffusion. Observations of the interaction between two nearly identical rings travelling a common path showed that, contrary to popular belief, rings do not pass back and forth through one another, but that the rearward one becomes entrained into the forward one. Only when the rearward ring has a much higher velocity than its partner can it emerge from the joining process and leave a slower-moving ring behind.

1. Introduction

The basic characteristics of vortex rings, as they are understood at the present time, are described in Lamb (1945), Prandtl & Tietjens (1934), Sommerfeld (1950) and Batchelor (1967) for example. More recently Saffman (1970) has reopened the discussion on the theoretical aspects of the problem and in particular, the effects of viscosity.

Elementary considerations show that there is a basic inconsistency between the classical models and even the most casual observations of the motions of real vortex rings. The latter show that the ring slows down and grows to larger overall diameter as time progresses. Kelvin's model (Lamb 1945, p. 241) has neither of these features. Saffman's (1970) extension of this picture allows the

initially thin core of vorticity to grow by viscous diffusion and a slowing of the ring is predicted. Thus

$$U = \frac{K}{2\pi r}\left\{\log\frac{8r}{(4\nu t)^{\frac{1}{2}}} - 0{\cdot}558 + O\left(\frac{\nu t}{r^2}\right)^{\frac{1}{2}}\right\}.\dagger \tag{1}$$

Because the core remains thin it is not possible for the circulation K to change. The impulse I of the ring is also constant and given by

$$I = \pi r^2 K. \tag{2}$$

However, observations show that r increases with time and a contradiction is reached if we wish to retain the thin-cored model. Either I must increase or K must decrease. The former is not possible because there are no body forces available to bring it about. The latter is also impossible unless, at least, we allow the size of the core to grow until vorticity is able to cancel, by viscous diffusion, at the centre-line of the ring. Saffman (1970), by order-of-magnitude arguments, calculated that

$$U \approx (I/k)\,(r_0^2 + k'\nu t)^{\frac{3}{2}}$$

for this circumstance, where r_0 is the initial radius of the ring and k and k' are constants. His model contains some of the features of the one to be described in the following sections; in particular, we find that the vorticity is not confined to a thin core in vortex rings produced by a simple vortex generator.

Reynolds (1876) appears to have been the first to observe correctly the flow field of a real vortex ring. He noted that they slow down and grow because "...they are continually adding to their bulk water taken up from that which surrounds them and with which their forward momentum has to be shared". Since that time, numerous experiments and various refinements in interpretation have been forthcoming. Most of these have been hampered by an incomplete knowledge of the flow field and have ignored the important result that Reynolds obtained.‡ As a result, misinterpretations have arisen which should be corrected. Recently there have been suggestions that vortex rings may be used to transport chimney wastes to great altitudes and that vortex rings may form from the trailing vortices behind aircraft and from flares in the solar atmosphere. All of this has created a need to perform more complete observations on experimentally produced rings. After performing the experiments described in the main body of this paper, it also becomes apparent that the observed entrainment process could be of great importance in understanding the mechanism by which turbulent interfaces grow and remain sharp. In fact, by regarding the vortex ring as a model turbulent eddy which, when it reaches the turbulent-laminar interface, is able to entrain fluid by a process involving viscous diffusion, a new attack on one of the more interesting aspects of turbulent motion might be possible.

† U and r are the velocity translation and radius of the ring, respectively. K is the circulation around the thin core, ν is the kinematic viscosity of the fluid and t the time.

‡ A paper by Krutzsch (1939), discovered during the preparation of the revised draft of this paper, also shows the entrainment process very clearly, but draws no conclusion as to the mechanisms causing it.

2. Apparatus

The apparatus used in the present experiment was very simple. It consisted (figure 1) of a $\frac{1}{2}$ in. diameter, sharp-edged hole drilled through a thin sheet of brass and connected through a manifold to a hypodermic syringe (figure 1 (*a*)) or a sheet-rubber percussion head (figure 1 (*b*)). This device was placed in a 12-gallon aquarium. The rings were produced by ejecting a puff of fluid through the hole and observed using dye and hydrogen bubbles. Of the experimental parameters at our disposal, viz. fluid viscosity, hole diameter and shape, volume of fluid displaced into the tank and time taken to displace this volume of fluid, only the last two were varied over a wide range. The hole diameter was doubled for one set of tests and an obstacle (figure 1 (*c*)) was placed in the centre of the hole for another set; no attempt was made to cover a wide range of exit conditions once the major features of the flow had been discovered.

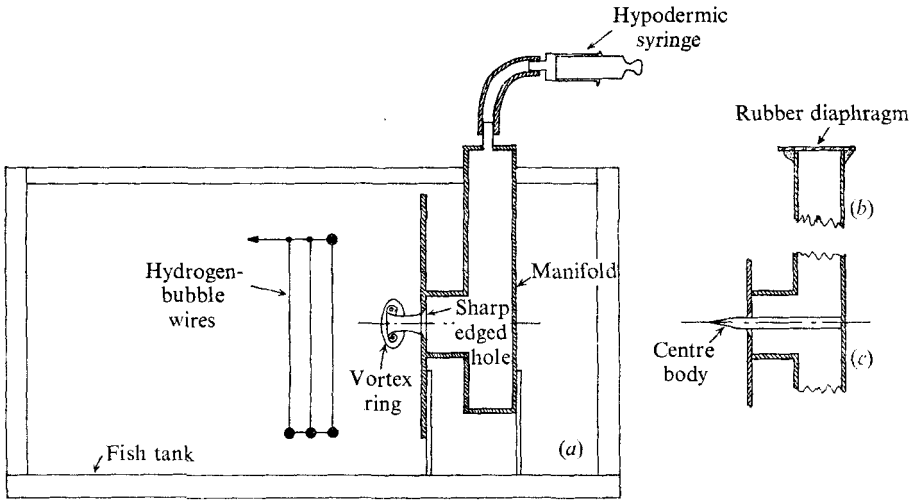

FIGURE 1. Apparatus. (*a*) Plunger, manifold and hydrogen-bubble wires installed in the aquarium. (*b*) Alternative form of device to apply an impulse to the ejected fluid; a rubber diaphragm is glued to the top of the manifold. (*c*) Alternative hole geometry with a centre body to test a stability criterion for the vortex rings.

3. Experimental results on laminar vortex rings†

Vortex ring formation was initiated by gently pushing the plunger of the syringe until a predetermined volume of fluid had been released. During this time a short jet of dyed fluid emerged from the manifold and immediately rolled up into a body of moving fluid which initially took the form of a oblate spheroid. Within this region the dye had deformed into a thin sheet with a spiral structure when viewed in a meridional plane. The dye sheet also closed over the nose of the region indicating a front stagnation point. Hydrogen-bubble pictures

† See §5 for a discussion of the circumstances under which such stable laminar rings can be formed.

(figure 2, plate 1) to be described in detail later, showed that the dyed sheets were not regions of concentrated vorticity† (Magarvey & MacLatchy 1964), but that the vorticity was distributed throughout the moving fluid body. As the ring moved away from the hole, the dye indicating the stagnation point disappeared and the ring grew in diameter with clear fluid in the central hole of the torus. This sequence has already been reported by Okabe & Inoue (1960) in an obscure location, while Batchelor (1967) has reproduced it for a wider audience. Figures 3(*a*), (*b*), (*c*) (plate 2) are photographs of the later stages of development of such a ring. Prandtl & Tietjens (1934) interpreted the dyed region to be the limit of the irrotational fluid which was moving with a thin vortex core (figure 3(*a*)). By introducing the dye into the path of the moving ring we can see that this statement is incorrect and produce the photographs shown in figures 3(*b*), (*c*) (plate 2). It is evident that the fluid volume moving with the ring‡ is considerably larger than the old dyed region and that *new fluid from upstream is being entrained into the rear of the bubble.*§ It rolls up around the old ring and pushes the boundary of the moving fluid outwards. The new dye also shows that a stagnation point still exists but that it has been moved forward from its original location. Measurements show that the ratio of maximum bubble diameter to length in the axial direction is constant to within experimental error. Thus the bubble has a similar shape as it propagates, even though the ring that was originally dyed is changing shape, becoming larger in overall diameter and smaller in cross-section. Figure 4(*a*) shows a diagrammatic view of the entrainment process. Drawing the streamlines for such a flow is difficult because the flow is doubly unsteady. It is translating with respect to an observer and the bubble is growing in size as time progresses. The first difficulty can be removed by moving along with the bubble. The second is harder to resolve. Figure 4(*b*) is an attempt to draw instantaneous streamlines for the *growing* bubble surface. It is clear that the dye 'streaklines' are not the same as the streamlines for this unsteady flow, and interpretation of the dye motion requires great caution.

Measurements of the bubble's velocity of translation U show that it decays exponentially with distance x_1 from the hole (figure 5).

Since $U \equiv dx_1/dt$, an elementary integration shows that

$$U \sim t^{-1},$$

where t is the elapsed time measured from the imagined start of the motion at a virtual origin at downstream infinity. The latter point may be difficult to understand but it should be realized that since the velocity varies exponentially with distance, it is the one case in which the bubble covers an infinite distance from the virtual origin in a finite time. This rather unusual, and apparently unique, situation is in contrast to previously studied cases of jets, plumes, etc., in which all quantities varied algebraically with distance and the virtual origin was a finite distance from the orifice creating the actual motion.

† The dyed sheet remained sharp because the diffusion coefficient of the dye particles was very small. In contrast, the vorticity produced by viscous separation at the sharp edge of the hole underwent viscous diffusion and was quickly smoothed.

‡ We will call this moving volume of fluid a 'bubble' in the following sections.

§ An observation which confirms Reynolds's (1876) original statement.

By introducing the impulse I of the ring and its circulation K, measured around the circuit shown in figure 9, it is possible to make several predictions. Assuming that I is constant, as it would be if no impulse were lost to a wake, then

(i) $I \sim Ua^3 = \text{const.}$ and hence $a \sim t^{\frac{1}{3}}$, while

(ii) $K \sim Ua \sim t^{-\frac{2}{3}}$, where a is a characteristic dimension of the bubble.

Measurements of $a(t)$ (figure 6), from a moving picture sequence, reveal that prediction (i) is closely realized. The second prediction is difficult to check directly, but its consequences can be observed. We will show in § 4 that the only way for sufficient vorticity to be removed from the bubble, in order to explain (ii),

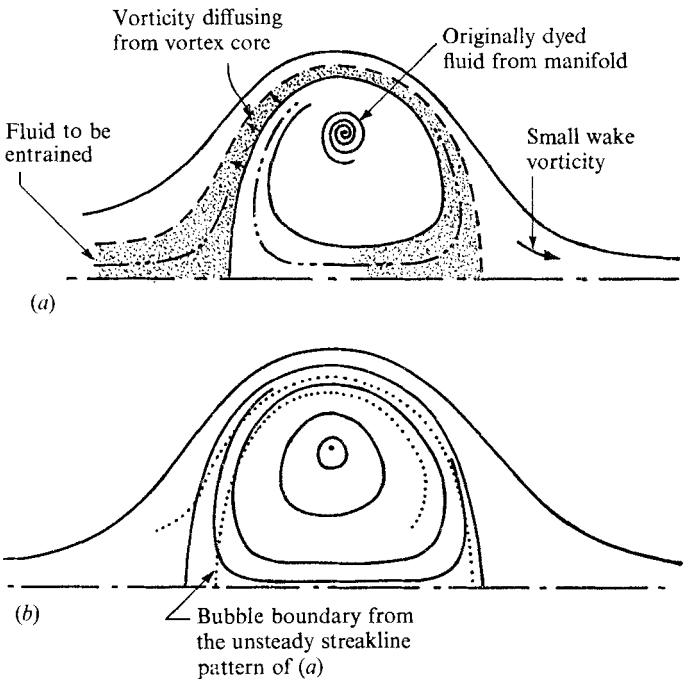

FIGURE 4. (*a*) Diagrammatic view of entrainment by a vortex ring, showing fluid from upstream being entrained into the outer regions of the ring. (*b*) Diagrammatic view of instantaneous streamlines in a frame of reference moving with the mean velocity U of the ring.

is for there to be a continuous rejection of ring vorticity into a wake. Before the evidence showing the existence of such a wake is presented, it should also be noticed that the velocity U decreases faster than exponentially when it becomes small (figure 5). It will also be shown in § 4 that this is probably due to the cumulative effects of the continuous rejection of impulse to the wake, together with the vorticity, and a corresponding decrease in the impulse of the ring.

Hydrogen-bubble pictures (figures 7 (*b*), (*c*), plate 3) reveal the existence of the predicted wake far behind the bubble.† In the expression for the wake azimuthal

† Chronologically, the existence of the wake was only suspected and then verified after the model developed in § 4 predicted that such a structure was needed in order to produce a dynamically consistent picture.

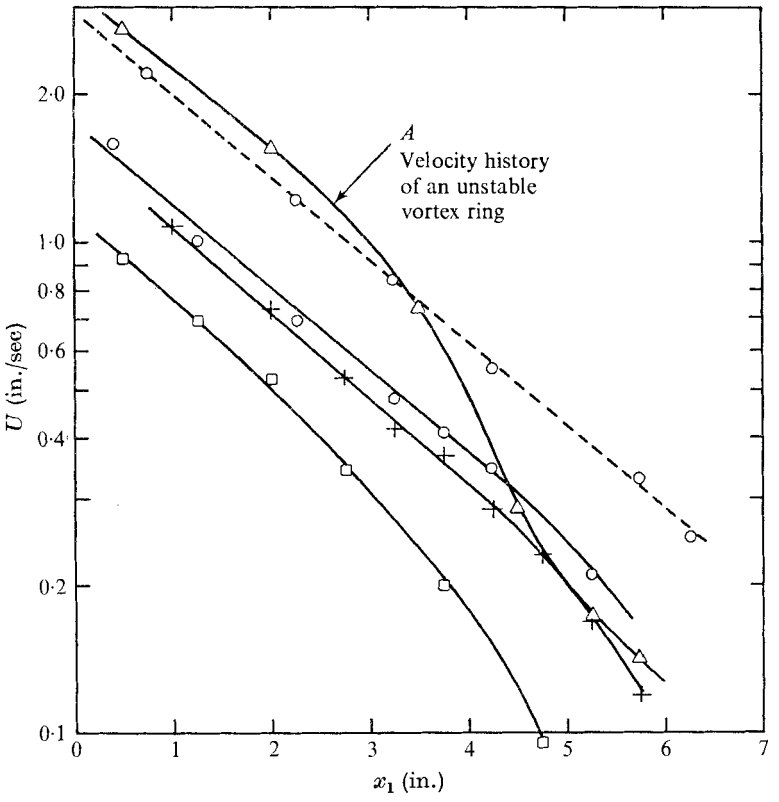

FIGURE 5. Velocity of translation of bubble U versus distance from the hole at which it was formed (x_1). All rings except A had an initial Reynolds number less than 600.

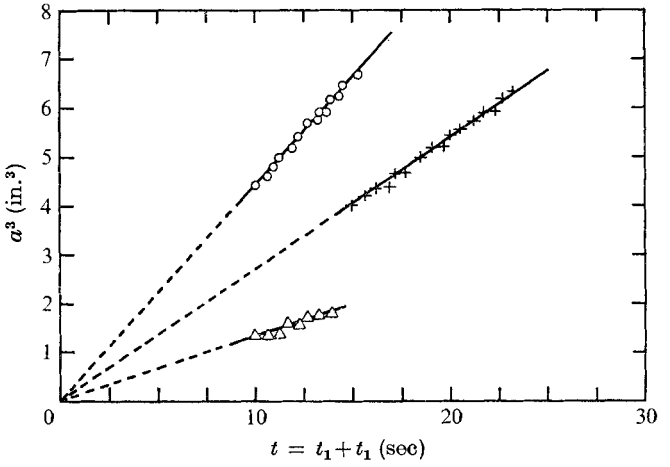

FIGURE 6. a^3 *versus* time t from the virtual origin of the motion. The time t consists of two parts. t_1 is the time measured from the start of the real motion at the hole. t_0 is the time that must be added to account for the motion between the virtual origin and the hole. In this case a is the diameter of the ring measured between the centres of rotation indicated by the dyed ring.

vorticity $-\partial u/\partial y$† can be measured directly from the hydrogen-bubble pictures. The second term, $\partial v/\partial x$,† can be estimated from the measured axial variation in u and the use of the continuity equation. Such calculations show that, even for most conservative assumptions, the second term is negligible and that a net azimuthal vorticity exists in the wake behind the moving vortex bubble. Based on previous knowledge, such a result is quite unexpected, but is needed so that a consistent dynamical picture results from all the observations. At this point it is not clear how we should further interpret these profiles. However, once the theory (of § 4) has been presented we will return to these results and in fact show that they support the theoretical model in a very satisfactory way.

Further evidence in favour of both entrainment and the wake is shown in figure 7 (*a*) (plate 3). There a vortex ring has been puffed from a reservoir containing no dye. A vertical curtain of dye, about one or two ring diameters wide, was spread four diameters ahead of the exit hole. As the undyed ring passed through the dyed region it entrained some dye and dragged still more along in its wake. A similar process is shown in figure 3 (*a*) (plate 2) where a red dye blob, shown behind and slightly above the centre-line of the blue dye of the ring, has been distorted by the flow field of the wake but not entrained. It was originally placed a little too far from the path of the ring and was not affected by that part of the vorticity which was re-entrained into the bubble. This explanation anticipates a fuller discussion of the physical mechanisms at work which follows after we have commented on the velocity field within the bubble itself.

Using hydrogen bubbles to observe the velocities within the bubble is not as accurate as using them to observe the wake. Substantial axial velocity gradients, and associated radial velocities, are present in the former case and make interpretation of the bubble-line distortions difficult. Several simple approaches were tried using figure 2 (*a*) (plate 1). All of these showed that vorticity was distributed continuously throughout the bubble volume, but that it was not distributed linearly with radial distance as required by the theory of Hill's spherical vortex (Lamb 1945) and O'Brien's (1961) generalization to spheroidal vortices. The vorticity distribution showed a distinctly smaller slope close to and at the axis than near the surface of the bubble. There was no indication that the vorticity was concentrated in a thin core, as suggested by the classical model reproduced in most text-books. It seems pointless to reproduce graphs showing the experimental distribution because the actual shapes are not accurate. We hope to repeat these measurements in the future using better techniques.

Based on these observations, we can now qualitatively describe the dynamical processes that we believe are important to an understanding of the flow. Then in the following section (§ 4) we present a theoretical model based on these processes and show that it can in fact predict the behaviour of the bubbles. The vorticity produced by viscous separation at the hole initially fills a bubble appropriate to the amount of fluid displaced and the impulse applied by the plunger motion. Fluid exterior to the manifold is entrained into the bubble during its formation; this process is described in more detail in § 5, where it plays an important part in determining the stability of the system. As the bubble

† u and v are velocity components in the axial x and radial y directions respectively.

moves away from the hole, at a velocity determined by its own self-induction, vorticity diffuses away from the bubble surface. Irrotational fluid flowing over the bubble surface picks up this vorticity, dissipation occurs and then the fluid has insufficient total pressure to flow completely over the bubble. In viscous flow over a solid surface, this vortical region would separate from the surface; in the present case it does not do so but is entrained into the rear of the bubble causing the bubble volume to increase.† Further from the bubble surface, where the vorticity has diffused to smaller values, the fluid particles traverse the bubble without being entrained and then have sufficient vorticity to be detectable as a wake. The shed vorticity accounts for the wake motion, but is far enough from the bubble to have little effect on its motion. In between, one surface comes to the rear stagnation point which separates entrained fluid from that which can flow over the body. The dynamical processes which decide the exact amount of shed vorticity can only come from detailed study of the flow near the rear stagnation point and such a study has not been attempted. Thus, we see that the velocity of translation is decreasing for several reasons. The available vorticity is being spread over a larger and larger bubble volume as time progresses, vorticity is being cancelled by diffusion across the axis of symmetry of the bubble and vorticity is being lost to a wake. These arguments are purely kinematic since the self-induction and hence velocity at any instant depends only on the amount and distribution of the vorticity in the system. This simple model also explains why the commonly observed dye ring is a very misleading flow marker which can only be used to indicate the velocity of translation of the ring and give a measure of the diameter, taken between the centres of rotation. The argument hinges on the fact that the diffusion coefficient of the dye particles (smoke particles in a ring produced by a cigarette smoker) is very much smaller than the diffusion coefficient for the vorticity, i.e. the kinematic viscosity. Thus, initially, as the vorticity diffuses away from the dyed spheroid the dye is left behind. Entrained fluid wraps around the dyed region and it remains trapped while vorticity is more rapidly diffused and convected away. Such a description also explains one of the differences between stable buoyant vortex rings produced by a rapidly diffusing buoyancy source, e.g. hot air moving in colder air, and a slowly diffusing buoyancy source, e.g. brine in fresh water. In the former case, the buoyancy is spread over the whole of the bubble since the heat and vorticity diffuse at essentially the same rate and a heated wake is formed. In the latter case, the heavy salty water remains in a thin ring which, although it is unstable, does not reach the outside edge of the bubble. A further paper on these aspects of the vortex ring problem is in preparation.

It is important to reiterate that in none of the situations considered did the vortex look like the classical thin vortex ring described in the literature. This statement was thought to be so controversial that many attempts were made to reproduce classical results. In order to do so, the hole diameter was enlarged and

† This process is similar to that described by Turner (1964) except that in his case the expansion rate of the bubble was set to agree with experimental observations and could, in fact, have been given any other arbitrary value. His flow was inviscid and independent of any entrainment 'mechanism'.

the top of the manifold was replaced by a rubber disk which when sharply struck, produced a ring of great velocity (an initial Reynolds number of about 20 000), with a very thin dyed region.† Superficially, this looked like the thin vortex described by the theory. However, detailed dye studies showed that this was not in fact so, and that the 'thin' ring was carrying a much larger fluid mass with it, was entraining more fluid and vorticity was being deposited into a wake all the time. It is concluded that thin rings cannot be produced by a generator such as ours except, perhaps, under conditions far more extreme than those studied here (i.e. at very large Reynolds numbers).

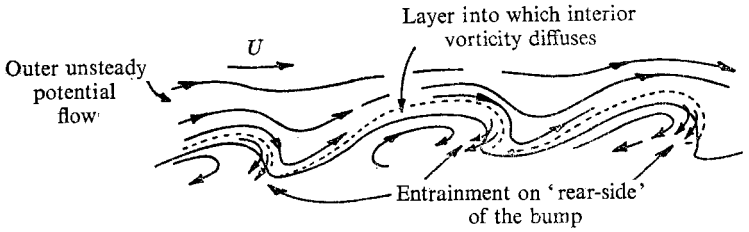

FIGURE 8. Diagrammatic view of the entrainment process which takes place at a turbulent interface.

One of the more important deductions derived from the present observations concerns the mechanism whereby turbulent interfaces entrain fluid and at the same time remain sharp. A turbulent interface is an unsteady corrugated surface over which an outer irrotational fluid flows and within which all of the vorticity is contained. Within the context of the present experiment one can see that as the vorticity diffuses across the interface into the irrotational fluid, the fluid thus affected can no longer flow over the surface and will be entrained on the backside of a corrugation (figure 8). Of course, the situation is not as clear as that for the vortex ring since the surface is both unsteady and three-dimensional, and consists of many scales all of which, except the very smallest, are able to entrain fluid. The velocity of the outer irrotational fluid, with respect to the surface corrugations, is also unknown and it would seem that it will be very difficult to put this process on a more quantitative footing. Now, at least, the mechanism of entrainment and sharpening can be understood in a qualitative way and may lead to more useful results at a later date.

4. A theory for stable laminar vortex rings

A simple dimensional analysis of the flow described in § 3 does not allow a unique determination of the dependence of bubble velocity and size on the elapsed time. In this section, we present a simple mechanistic theory which is essentially one step beyond such an analysis. The required addition is to model the entrainment of new fluid into the moving region of vorticity (figure 9(*a*)).

† This is the method originally used by P. G. Tait to demonstrate vortex ring phenomena to Lord Kelvin and resulted in the latter's development of the 'vortex-atom' theory of the properties of materials.

We are then able to determine the dependence of the size of the region on time. Three basic assumptions are required. The first is that the bubble remains similar at all times, so that the constants of proportionality which are introduced do in fact remain constant. The second requires that the vorticity be continuously distributed throughout the bubble, while the third requires that, initially at least, no vorticity be shed into a wake, with the consequence that the impulse of the ring remains constant. From this model we determine an inconsistency

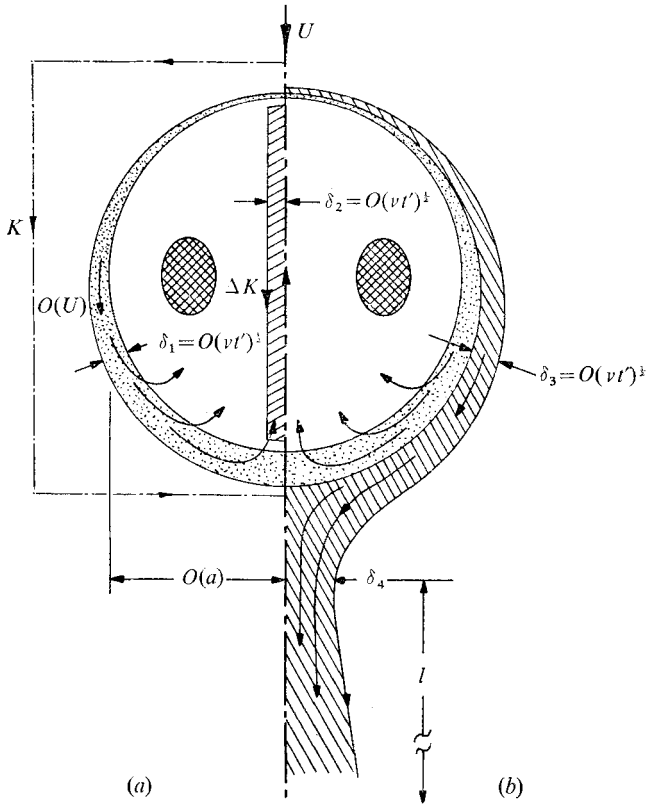

FIGURE 9. Entrainment model of a homogeneous vortex ring, where t' is a measure of the time it takes a particle to traverse the distance from the front stagnation point to the region of entrainment. (*a*) A first model with no wake and all diffused vorticity entrained. (*b*) A second dynamically consistent model in which some vorticity is deposited into a wake and some entrained back into the ring.

which can only be resolved by allowing the existence of a wake into which ring vorticity can be deposited (figure 9(*b*)). At this point it is critically important that the role of the bubble impulse† is correctly interpreted. The total impulse imparted to the system cannot change (Batchelor 1967, p. 520). Initially, it is all contained within the bubble. As time progresses and vorticity is placed in the

† The impulse is given by $\frac{1}{2}\rho\int \mathbf{x}\times\boldsymbol{\omega}\,dv$; where $\mathbf{x}$ and $\boldsymbol{\omega}$ are the position and vorticity vector respectively, and dv an element of volume. In principle, the integral is taken over the whole fluid, but it obviously need only be taken over the region where there is vorticity. This impulse applied to a *limited fluid volume* generates the *whole* of the fluid motion from rest.

wake, the total impulse is shared by both the bubble and the wake. The impulse responsible for the bubble motion is continuously decreasing while that responsible for the wake motion is continuously increasing.† However, it is possible to show that the assumption of constant bubble impulse is still satisfactory when the Reynolds number of the bubble is large and the elapsed time short. Ultimately, the loss of bubble impulse becomes important and invalidates our simple model, but this occurs only after a long time and after the Reynolds number has decreased to small values.

We start the detailed analysis by reference to figure 9(*a*), which shows the entrainment process diagrammatically. As the vorticity diffuses from the bubble interior, it contaminates a thin layer of initially irrotational fluid, dissipation occurs, the total pressure in the layer is slightly reduced and it is unable to traverse the bubble contour. As a result, the layer is entrained into the bubble interior bringing the diffused vorticity with it. At the point where the layer is entrained into the bubble, it has a thickness $\delta_1 = C_1(\nu t')^{\frac{1}{2}}$ and velocity $C_4 U$, where $t' = C_2 a/U$ is the time for a particle to traverse the distance around the bubble and ν the kinematic viscosity of the fluid. The circumference of the entrained region is $C_3 a$. Thus, the rate of change of bubble volume V equals the amount of fluid entrained per unit time,

$$\begin{aligned} dV/dt &= C_1 C_3 C_4 a U (\nu t')^{\frac{1}{2}} \\ &= C \nu^{\frac{1}{2}} a^{\frac{3}{2}} U^{\frac{1}{2}}, \end{aligned} \tag{3}$$

where $C = C_1 C_3 C_4 C_2^{\frac{1}{2}}$. The impulse is constant and given by

$$I = \alpha K a^2. \tag{4}$$

The velocity of propagation is given by

$$U = \beta K/a = \beta I/\alpha a^3, \tag{5}$$

where α and β are constants which depend on the bubble shape. Substituting into (3) gives finally

$$dV/dt = A(\nu I)^{\frac{1}{2}} = \text{constant}, \tag{6}$$

where $A = C(C_2\beta/\alpha)^{\frac{1}{2}}$. Integration of (6) gives

$$V \equiv Ba^3 = A(\nu I)^{\frac{1}{2}} t + D, \tag{7}$$

where B is another shape dependent constant. The constant D is evaluated by using the initial condition that $V = 0$ when $t = 0$, so that $D = 0$. It then follows that

$$\left.\begin{aligned} a &= (A/B)^{\frac{1}{3}} (\nu I)^{\frac{1}{3}} t^{\frac{1}{3}}, \\ U &= (\beta B/\alpha A)\,(I/\nu)^{\frac{1}{2}} t^{-1}, \\ \text{and} \quad K &= aU/\beta = (B/A)^{\frac{2}{3}} \alpha^{-1} (I^2/\nu)^{\frac{1}{3}} t^{-\frac{2}{3}}. \end{aligned}\right\} \tag{8}$$

This result agrees with the measurements of $U(t)$ and $a(t)$. Thus in order to maintain the impulse constant, the observed increase in a is accompanied by a

† Note that once the impulse (vorticity) has entered the wake it still has some effect on the motion of the bubble; this effect becomes small beyond about one diameter from the bubble.

decrease in K as distinguished from previous models. It is now necessary to find a consistent mechanism to explain this decrease. Within the present model, the only place that it can occur is at the axis of symmetry. There the vorticity is diffusing and cancelling over a region which has a width $O(\delta_2)$ and a length $O(a)$ (figure 9(*a*)). Within this region the vorticity is $O\{(U/a)\,(\delta_2/a)\}$. Thus, the circulation cancelled by diffusion within the small circuit ΔK is

$$\Delta K \sim \frac{U}{a}\frac{\delta_2^2}{a^{\frac{1}{2}}}a.$$

The time over which this loss takes place is $O(a/U)$, so that

$$\frac{dK}{dt} \sim \frac{U\delta_2^2}{a}\frac{U}{a} \sim \left(\frac{U}{a}\right)^{\frac{3}{2}} \sim t^{-\frac{4}{3}}$$

or

$$K \sim t^{-\frac{1}{3}}, \tag{9}$$

which does not agree with the result found from the entrainment model. The same result is found using an equation given by Saffman (1970) for the change in circulation close to the centre-line

$$\frac{dK}{dt} = \nu\int_{-\infty}^{\infty}\left(\frac{\omega}{y}\right)_{y=0}dx. \tag{10}$$

Substitution gives

$$dK/dt \sim aU/a^2 \sim t^{-\frac{4}{3}}, \tag{11}$$

where ω is the vorticity and y distance from the centre-line. We are thus faced with a dilemma which can only be resolved by increasing the internal vorticity gradients (which are not observed) or by allowing the vorticity to be convected out of the bubble and for the diffusion and cancellation to then take place over a much longer distance, i.e. in a wake. As already mentioned, the main difficulty in allowing such a structure is to explain how the assumption of constant impulse still describes the flow even though the bubble impulse is left behind in the wake.

We now turn to the revised model shown in figure 9(*b*). The entrainment argument proceeds as before and gives the same results although the constants may have different values. Now, however, we allow some vorticity of $O(U/a)$ and its associated circulation to be shed into a wake of width δ_4 from a thin layer of width $\delta_3(= C_5(\nu t')^{\frac{1}{2}})$. Thus the rate of change of circulation is given by

$$\frac{dK}{dt} \sim \frac{U}{a}\delta_3 a\Big/\frac{a}{U} \sim \frac{U^{\frac{3}{2}}}{a^{\frac{1}{2}}} \sim t^{-\frac{5}{3}}$$

or

$$K \sim t^{-\frac{2}{3}}, \tag{12}$$

which is now consistent with the results of the entrainment model. This circulation in turn is deposited into the wake where it ultimately diffuses and cancels over a length l, so that by applying (10) to the wake region, we find

$$dK/dt \sim \nu l\omega/y. \tag{13}$$

It seems reasonable to suppose that, since the curl of the vorticity (ω/y) is coming from vorticity deposited into the wake from the outer regions of the bubble,

$$\omega/y \sim U/a^2. \tag{14}$$

Thus from (12), (13) and (14),

$$l \sim a(Ua/\nu)^{\frac{1}{2}} = aR^{\frac{1}{2}},$$

where R is the bubble Reynolds number Ua/ν.

Associated with the deposition of vorticity is a deposition of impulse into the wake which in turn results in a small decrease in the impulse of the bubble alone. We calculate the characteristics of the wake under the assumption that the bubble impulse is constant, a procedure which can only be valid while the accumulated wake impulse is small. Comparison with the experimental results suggests that this is a reasonable approximation for high ring velocities and short times after ring formation.

The increment of impulse (ΔI_w) residing in a short section of the wake of length ΔX is given by

$$\Delta I_w \sim \Delta X \int_0^{\delta_4} \omega y^2 \, dy; \tag{15}$$

where ω comes from equation (14). Substitution of (14) into (15) followed by integration and taking the limit $\Delta X \to 0$ yields

$$dI_w/dx \sim U\delta_4^4/a^2.$$

Assuming that $\delta_4 \sim aR^{-n}$, as suggested by the solution to the related problem of an immiscible fluid bubble moving in another fluid (Harper & Moore 1968), then

$$dI_w/dx \sim Ua^2/R^{4n}. \tag{16}$$

The impulse found in the wake has been shed from the bubble. By using an argument that is virtually identical to that used to calculate the shedding of vorticity into the wake, we can find the amount of impulse left in the wake

$$dI_w/dx \sim \nu^{\frac{1}{2}}U^{\frac{1}{2}}a^{\frac{3}{2}} \sim \nu^{\frac{1}{2}}I^{\frac{1}{2}} = \text{constant}. \tag{17}$$

Comparison of equations (16) and (17) shows that

$$n = \tfrac{1}{8}.$$

Equation (17) can be integrated to give

$$I_w = I_0 + b\nu^{\frac{1}{2}}I^{\frac{1}{2}}x_1, \tag{18}$$

where I_w is the total impulse residing in the whole of the wake to the point x_1; I_0 is the wake impulse up to the hole itself and b a constant. Since the real bubble was actually formed at the hole, i.e. $x_1 = 0$, it starts out with the given impulse, I, and no wake, so that $I_0 = 0$. Thus, after the bubble has travelled a distance $x_1 = ma$ then,

$$I_w/I \sim m/R^{\frac{1}{2}}, \tag{19}$$

which is small when R is large and m is small. It is suggested that this loss of impulse to the wake accounts for the departure of the measured values of $\log U$ *versus* x_1 (figure 5) from a straight line when m has become large and R small. It is also possible that at such low values of R the boundary-layer approach used here becomes invalid and also contributes to the departure from the proposed model.

Unfortunately, the proposed model has a rather limited range of applicability. It cannot be a correct dynamical description of the flow between the virtual origin and $x_1 = 0$ because the wake impulse is negative and actually approaches $-\infty$ as $x_1 \to -\infty$. However, we force this imagined bubble to pass $x_1 = 0$ with no wake impulse and the correct values of I, K, a and U. For a short distance, it is a good description of the real flow because as we have shown, the loss of impulse from the real bubble should be small and our constant impulse model agrees with experimental results. After some time has elapsed, however, the accumulated loss of impulse from the real bubble becomes too great and the model is no longer adequate. A correctly formulated model should take this loss into account, but such an effort is beyond the scope of this paper.

Figure 7(*b*) (plate 3) presents verification of one more piece of this picture. Our simple theory predicts that $dI_w/dx =$ constant, so that in each small section of the wake, of length ΔX, the increment of impulse is the same. Formation of the integral

$$\Delta I_w = \pi\rho\Delta X \int_0^{\delta_1} \frac{\partial u}{\partial y} y^2 \, dy$$

for each of the velocity profiles of figure 7(*b*) shows that ΔI_w is the same for each, to within 15%. Such a variation is well within experimental error for the hydrogen-bubble method used at such low velocities ($\sim$ 3 mm/sec).

Of passing interest is application of these ideas to a two-dimensional line vortex pair for which we find

$$a \sim (\nu I)^{\frac{1}{5}} t^{\frac{2}{5}},\dagger$$
$$U \sim (I^3/\nu^2)^{\frac{1}{5}} t^{-\frac{4}{5}},$$
$$K \sim (I^4/\nu)^{\frac{1}{5}} t^{-\frac{3}{5}}.$$

This result has obvious applications to the motion of the trailing vortices behind aircraft which could eventually interact in the way suggested here. It is also possible to predict the linear growth of buoyant vortex rings; this subject is to be reported in a subsequent paper.

5. Stability of vortex rings

When a circular ring of organized vorticity was puffed from the hole several possible histories could result depending on its initial size and velocity, i.e. Reynolds number, $R_0 = U_0 a_0/\nu$.‡

At low R_0 the motion was stable and the ring continued with a circular shape until it reached the end of the test tank (these were the rings studied in §§ 3 and 4). At $R_0 \gtrsim 600$ the circular bubble developed an azimuthal waviness with five peaks and five troughs (figures 10(*a*), plate 4). This waviness persisted more or less steadily while dye, and hence vorticity,§ was dragged from the peaks and into the wake (figure 10(*b*)). The velocity of the ring decreased rapidly during this

† In this case, I is the impulse per unit length of the vortex pair.

‡ Where U_0 is the initial velocity of translation and is of order K/a_0; a_0 is a representative length for the bubble (in this case its maximum diameter).

§ Since we have shown that the region of vorticity is outside and includes the dyed region, when dye is left behind vorticity must be also.

process and no turbulence was observed. For slightly higher values of R_0 the wavy structure collapsed into a turbulent blob and the vorticity was effectively cancelled by turbulent diffusion. At still higher values of $R_0 (\gtrsim 10^3)$ a new and more unexpected phenomenon appeared. The initial flow became unstable and broke into a turbulent motion which persisted for a short time. From this apparently disorganized vorticity field, a new vortex ring was formed (figure 10(*c*) plate 4). It was larger than the original ring and moved at a slower rate. Curve A of figure 5 shows the velocity history of such a ring.† Considerable amounts of

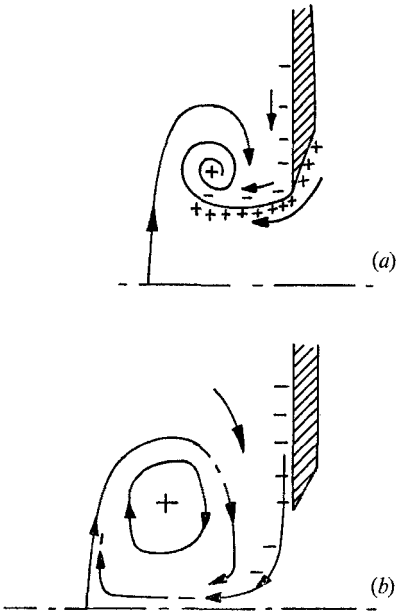

FIGURE 11. Ring formation at a sharp-edged orifice, showing production and convection of vorticity of the opposite sign (−) to that in the main body of the ring (+). (*a*) During outflow from the orifice. (*b*) After outflow has ceased and the bubble is beginning to close off.

dye and vorticity were left behind and redistributed during the breaking-up process and the state reached was apparently appropriate to a bubble of smaller initial Reynolds number.

Observations of the rings produced from the apparatus fitted with the rubber 'drum-head' showed, in fact, that the large rapidly moved rings were produced from such a mechanism. The original vorticity field emerging from the hole immediately broke up and the new stable vortex was born from this process. Large quantities of dye (and vorticity) were ejected radially outward from the nascent ring and were left behind. Evidently, such a simple ring is a poor device for transporting dye (pollution) to large distances. The new vortex had a Reynolds number of several thousand (typically 2×10^4) but was stable, whereas the vortex produced immediately at the hole became unstable for $R_0 \gtrsim 600$. One immediately

† Krutzsch (1939) shows that the stable rings formed from the initial instability also have velocities which decay exponentially with distance and are therefore described by the theory of §4.

suspects that the actual vorticity distribution produced by flow out of the sharp-edged hole is different and in some way more unstable than that produced after break up and reformation. The accuracy required to make this determination quantitatively can only come from better techniques than those used here and has not yet been attempted. However, it is possible to perform simple tests based on intuitive guesses about the mechanisms responsible for the instability. Simply, with the centre body (figure 1 (*c*)) in place, out-flow from the hole creates a core of vorticity of opposite sign from that of the main vortex ring. This vorticity is transported to the outside of the ring where it forms a layer which is unstable because the square of the circulation decreases rapidly outwards (Rayleigh's criterion). Under conditions which previously produced a stable vortex flow with no centre body the motion now became violently unstable, considerable vorticity was shed, and a new stable vortex emerged from the unstable region (figure 3 (*d*), plate 2†). It is suggested that in the process of forming a simple vortex ring (i.e. no centre body) vorticity of the opposite sign is created at the outside wall of the plate and this is swept into the vortex to ultimately create an unstable layer on the outside of the ring. The process is illustrated in figure 11. The photograph in figure 12 (plate 5) shows how the fluid from the wall and from the interior wrap around each other during the formation process and how the final process, by which the bubble is pinched off and leaves the neighbourhood of the wall, produces an outer layer which has opposing vorticity. The production of positive vorticity has ceased while the production of negative vorticity has not, since it is created by the motion of the vortex itself.

6. Interaction between two vortex rings

Since the present results lead one to suspect all the previous statements on single vortex rings, it seems proper to examine what really happens when two rings interact with one another. Current belief is contained in Sommerfeld (1950), for example, who devotes two pages (pp. 164–165) to a discussion of the possible interaction between two similar vortices moving along a common axis of symmetry. Owing to their mutual interaction, the rearward ring becomes smaller and moves faster while the forward one becomes larger and moves slower. The former can then pass through the latter. Thereafter, their roles become reversed and they oscillate back and forth through each other. Batchelor (1967, p. 524) states that "it is possible to demonstrate in the laboratory one or two such passages of one vortex through the other before they decay". The present author has been unable to repeat this experiment and, in fact, found results which did not agree with the textbook descriptions.

When two rings, of similar strenth, and R_0 less than 600, were puffed into the aquarium (figure 1), the rearward one became distorted by the velocity field (including the wake) at the forward one and squeezed into it through the rear stagnation point. It then wrapped itself around the inner ring to form a *single* large vortex. This sequence is shown in figure 10 (*d*) (plate 4). When the velocity

† Note the similarity to the unstable flow produced by flow out of the open hole (figure 10 (*c*), plate 4).

of the following ring was made larger than the leader, its entry caused the combined ring to execute longitudinal vibrations. Still larger velocities caused the combined ring to rip apart with a faster ring going ahead leaving a slower ring behind. It seemed as though the preceding ring actually gained some vorticity from the encounter because the trailing ring was moving slower than before. Evidence from analysis of moving picture sequences bears out this statement, but the exact amount of gain is hard to determine and then relate to the initial parameters.

The entrainment mechanism also explains the behaviour of interacting rings under other circumstances. When two rings were puffed out simultaneously along parallel paths they grew unaffected by each other until they just touched. Then any slight initial asymmetry caused one of the rings to entrain the closest edge of the other. The vorticity within these opposing regions was rapidly cancelled by diffusion over a thin region forming a single distorted ring which, under the action of its own induction, usually broke up into a turbulent blob.

T. Fohl (private communication) has projected rings at one another at various angles and found one very curious result. If the rings originally approached in one particular plane (the x, y plane for example, where the x direction is the average direction of motion of the two rings) they interacted and departed at approximately the same angles but in the x, z plane, i.e. a plane at right angles to the original. An explanation in terms of the entrainment model is quite easy. When they touch, the vorticity in each ring is cancelled locally, by the entrainment and subsequent diffusion, and leaves a single distorted ring. This ring, under the action of its own velocity field, distorts very rapidly to a new shape. The distortion is violent enough to cause the combined ring to split apart into two new rings moving in the observed directions.

7. Conclusions

From observations of the vortex rings produced by a simple generator, it has been found that stable rings exist in two ranges of initial Reynolds number (R_0). When $R_0 \lesssim 600$ the ring is stable during the whole of its motion. When $R_0 \gtrsim 1000$ the ring first of all becomes unstable, but out of the disorganized flow so formed, a new stable vortex emerges. Rings with very large $R_0 (\sim 2 \times 10^4)$ become unstable immediately after they are formed. The stable ring which emerges leaves behind most of the dye originally ejected from the generator. Such stable rings have several features not found in the usual text-book descriptions. Vorticity is spread throughout the body of fluid which moves with the dyed ring. The moving body of fluid is continuously entraining new fluid from outside and growing in volume, at the same time it is depositing its own vorticity into a wake. The present results, and those of Krutzsch (1939), show that the velocity of propagation of such stable rings varies exponentially with distance. A simple viscous entrainment model, in which the impulse of the moving fluid body remains constant, can describe most of the features of the observed flow. It only becomes inadequate after the impulse which is being shed continuously into the wake accounts for an appreciable fraction of the initial impulse of the

ring. For the intermediate range $600 \lesssim R_0 \lesssim 1000$, the vortex rings become unstable in a laminar fashion at the lower end of the range and as a disorganized turbulent region at the upper end. When two rings of closely similar velocity are moving along the same path, they do not pass through one another, as has been extensively reported, but the rearward one becomes entrained into the forward one to form a single large vortex. When the rearward ring has a larger velocity than the forward one, the combined ring becomes distorted and two rings can be reformed by the severance of vortex lines. The forward ring is now the faster and moves away from its mate.

A moving picture film has been produced to demonstrate the processes put forth in this paper. It is available on request to interested readers. Many fruitful discussions with Dr P. G. Saffman of the California Institute of Technology and Dr D. W. Moore of Imperial College are gratefully acknowledged. In fact, it was they who originally pointed out the fundamental role played by the wake and the similarity to the flows over liquid spheres studied at length by Harper & Moore (1968). Mr P. D. Weidman helped with the experiments and discussions with Mr E. J. Hinch helped formulate the theoretical problem. This work was supported at the University of Southern California by the National Science Foundation through Grant GK 2731 and at the Woods Hole Oceanographic Institution during the 1970 Geophysical Fluid Dynamics Programme. The generosity of Dr W. V. R. Malkus in providing a salubrious home during this latter period is gratefully acknowledged.

REFERENCES

BATCHELOR, G. K. 1967 *An Introduction to Fluid Dynamics*. Cambridge University Press.

HARPER, J. F. & MOORE, D. W. 1968 The motion of a spherical liquid drop at high Reynolds number. *J. Fluid Mech.* **32**, 367.

KRUTZSH, C.-H. 1939 Über eine experimentelle beobachtete Erscheinung an Wirbelringen bei ihrer translatorischen Bewegung in wirklichen Flüssigkeiten. *Ann. Physik*, **35**, 497.

LAMB, H. 1945 *Hydrodynamics*. Dover.

MAGARVEY, R. H. & MACLATCHY, C. S. 1964 The formation and structure of vortex rings. *Can. J. Phys.* **42**, 678.

O'BRIEN, V. 1961 Steady spheroidal vortices – more exact solutions to the Navier-Stokes equation. *Quart. Appl. Math.* **19**, 163.

OKABE, J. & INOUE, S. 1960 *Rep. Res. Inst. Appl. Mech. Kyushu U.* **8**, 91.

PRANDTL, L. & TIETJENS, O. G. 1934 *Fundamentals of Hydro and Aeromechanics*. Dover.

REYNOLDS, O. 1876 *Nature*, **14**, 477.

SAFFMAN, P. G. 1970 The velocity of viscous vortex rings. *Studies Appl. Math.* **49**, 371.

SOMMERFELD, A. 1950 *Mechanics of Deformable Bodies*. Academic.

TURNER, J. S. 1964 The flow into an expanding spherical vortex. *J. Fluid Mech.* **18**, 195.

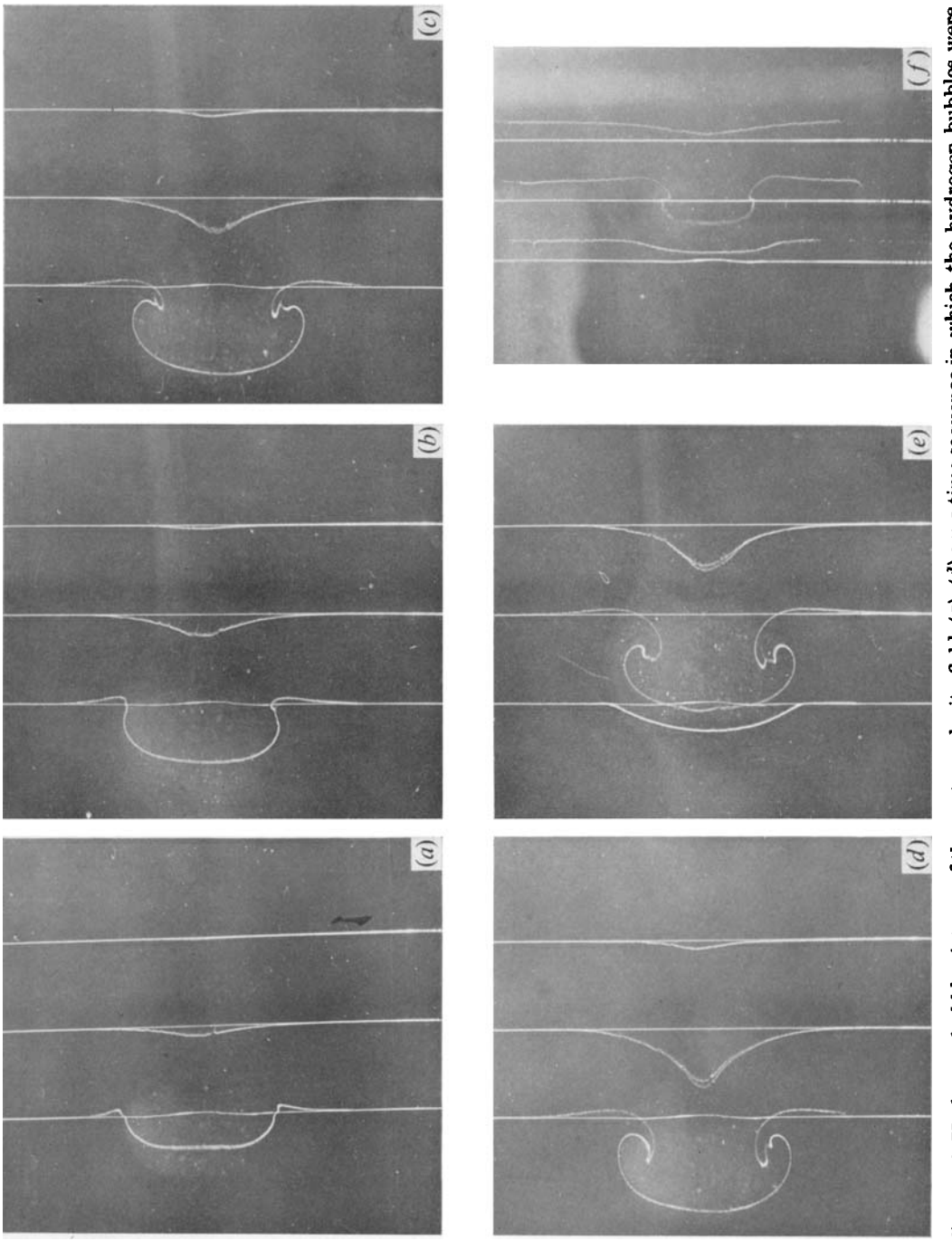

FIGURE 2. Hydrogen-bubble pictures of the vortex velocity field. (*a*)–(*d*) are a time sequence in which the hydrogen bubbles were formed as the centre of the vortex ring passed the last wire. The photographs (*a*)–(*d*) were taken at increasing times after hydrogen-bubble formation. (*e*) Same except bubbles were formed as ring passed the middle wire. (*f*) The wires were moved to keep the middle wire in the centre of the ring. Bubbles were formed and the photograph taken a short while later. Ring motion is from right to left in all cases.

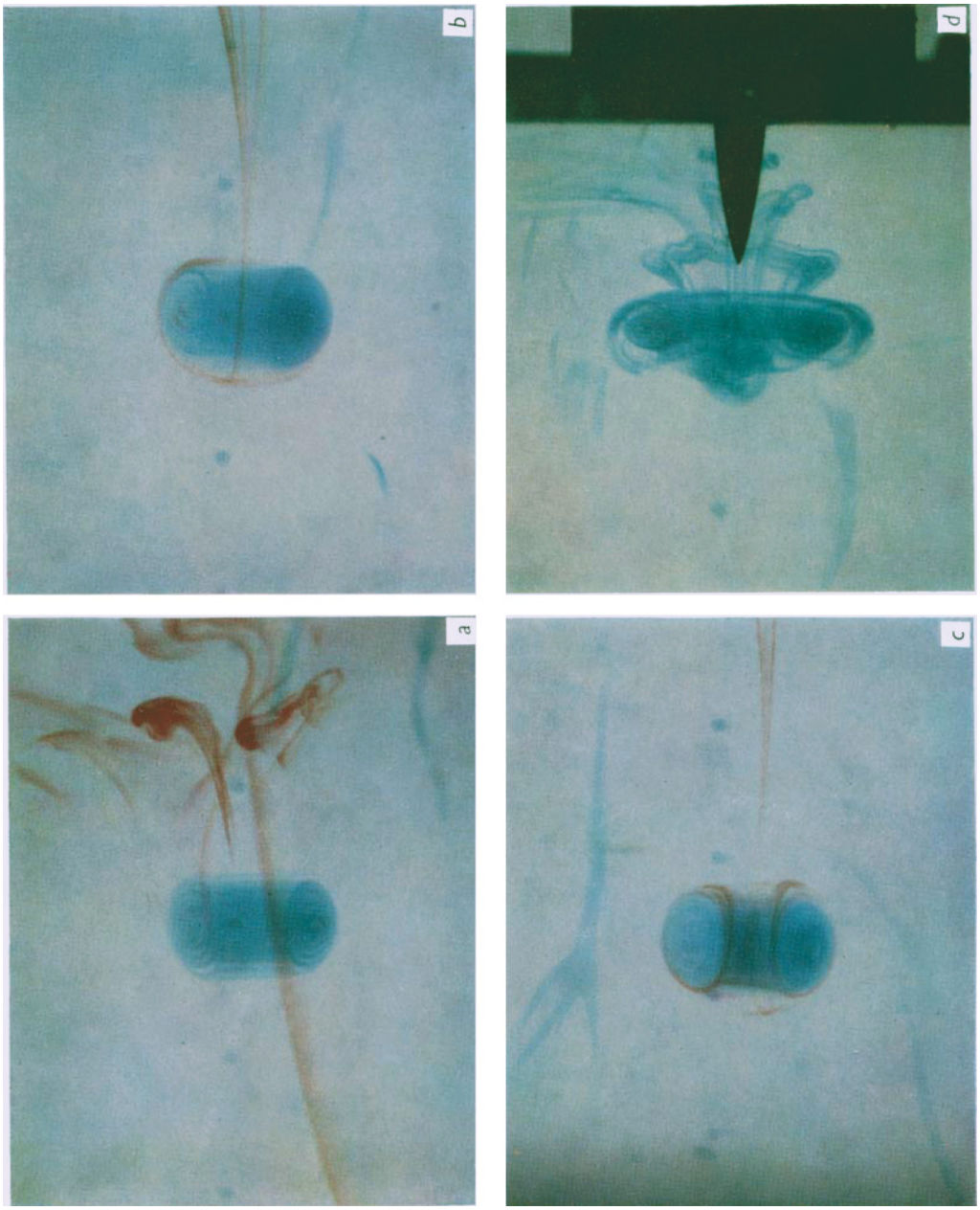

FIGURE 3. (*a*) Vortex ring approximately 8 ring diameters downstream from the hole. Clear fluid has been entrained into the centre of the ring and the ring has missed the red dye which had been placed in the tank. The dyed region is shaped like a torus. (*b*), (*c*) Same as (*a*) except that the original blue vortex has passed through a region of red dye. Entrainment of this originally irrotational fluid around the original dye region is evident. The fluid volume moving with the ring is larger than the doughnut shaped ring. (*d*) Instability of ring in which vorticity of opposite sign is produced by a centre body. Ring motion is from right to left in all cases.

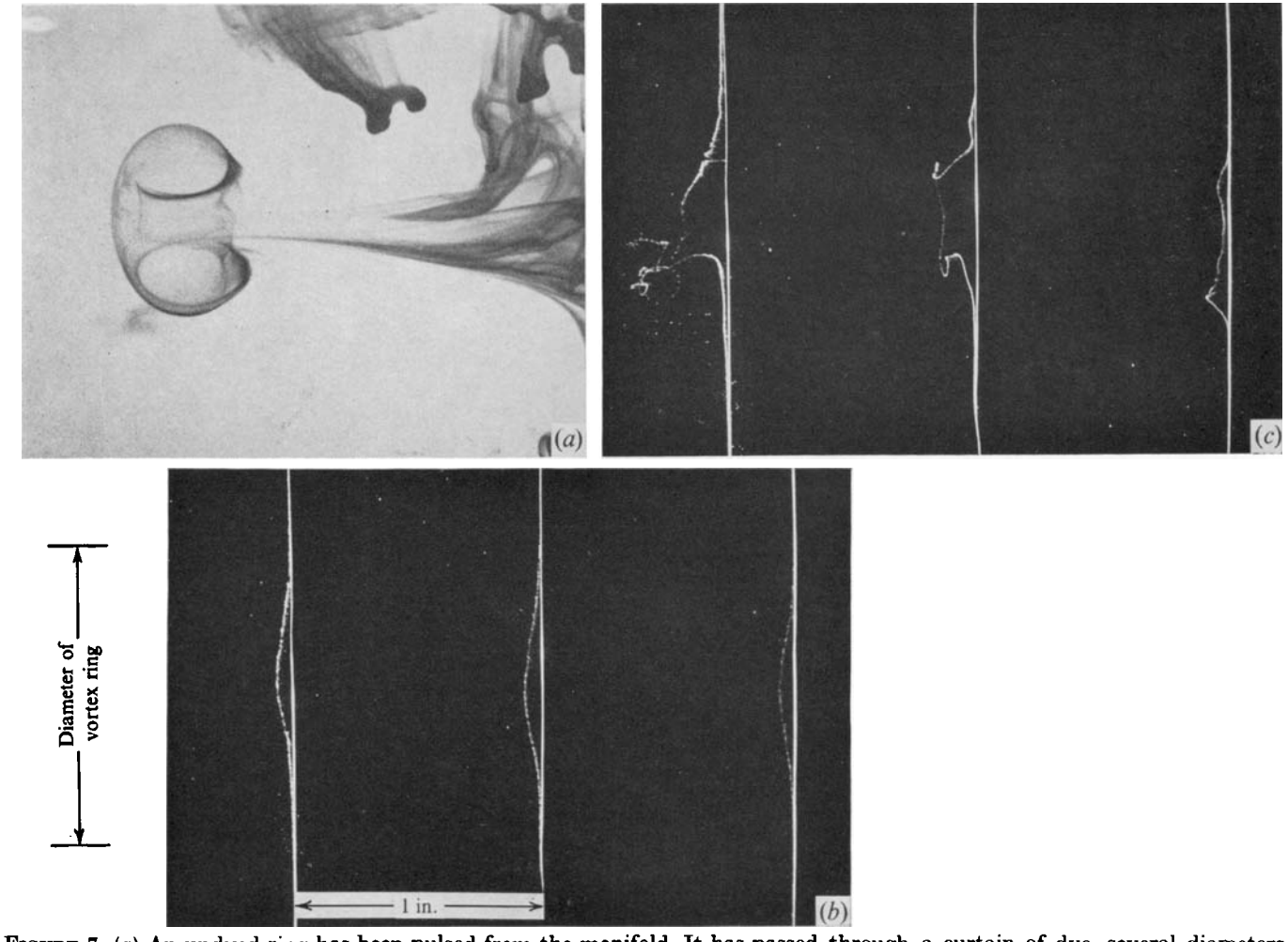

FIGURE 7. (*a*) An undyed ring has been pulsed from the manifold. It has passed through a curtain of dye, several diameters ahead of the exit hole. Dye has been entrained into the ring and has been dragged along in the wake behind the ring. (*b*) Hydrogen-bubble picture of the laminar wake behind a stable ring ($R_0 \sim 400$). Maximum velocity is approximately one-tenth of bubble velocity. (*c*) The turbulent wake behind an unstable ring ($R_0 \sim 800$). Maximum velocity is approximately one-half of the bubble velocity. In both cases (*b*) and (*c*) the ring has passed from right to left through the wires and was 3 diameters beyond the left-hand wire when the photographs were taken. The right-hand wire was 3 diameters from the hole forming the ring.

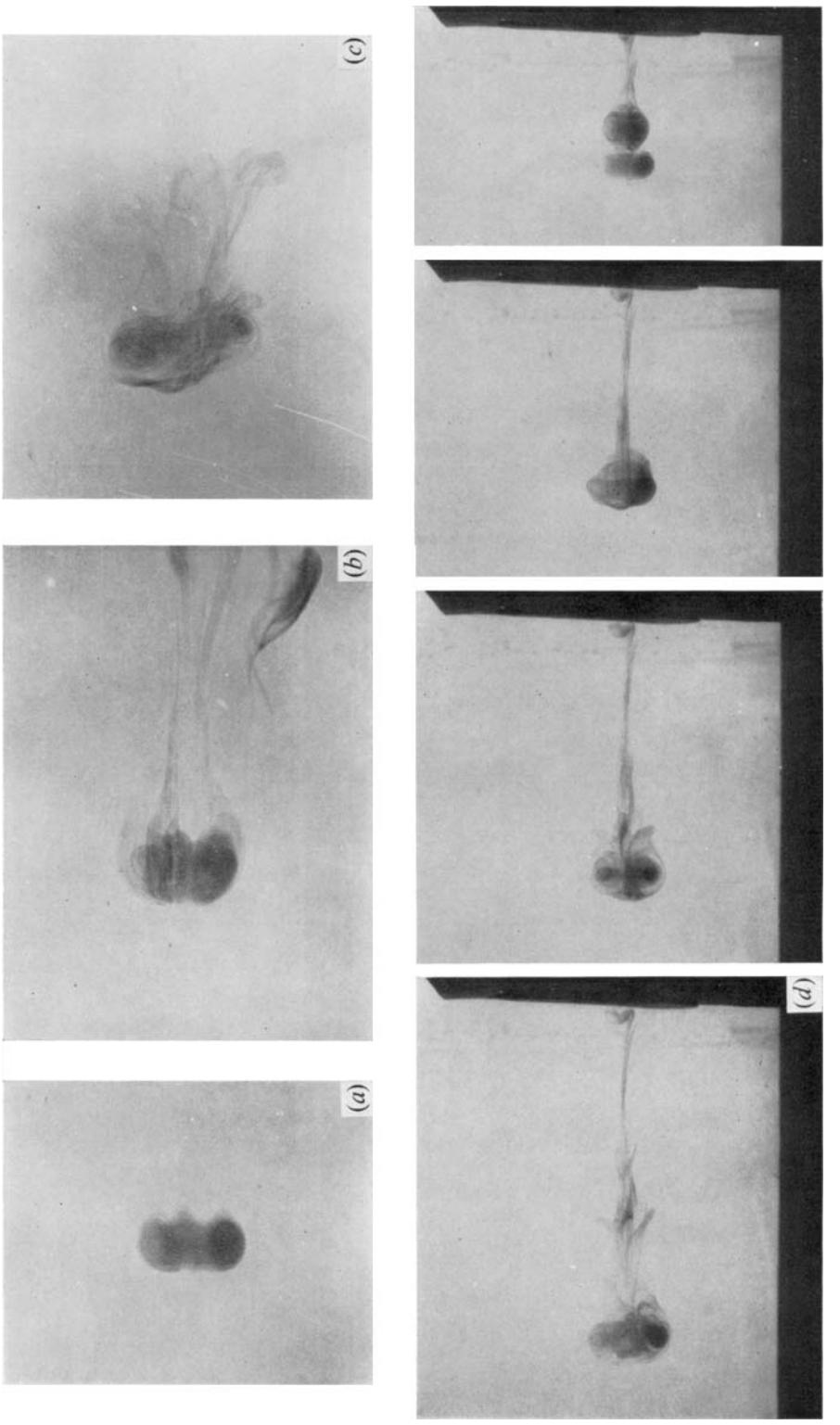

FIGURE 10. (*a*), (*b*) Azimuthal instability of the vortex ring produced by a sharp-edged orifice, showing in (*a*) five waves in the azimuthal direction and in (*b*) the deposition of dye into a wake. (*c*) Instability of the original ring followed by rebirth of a new ring from the unstable volume so formed, a great deal of dye has been left behind in a slowly moving ring-like structure. (*d*) Two rings moving on a common path. The rearward one is entrained by the forward one to form a single larger ring.

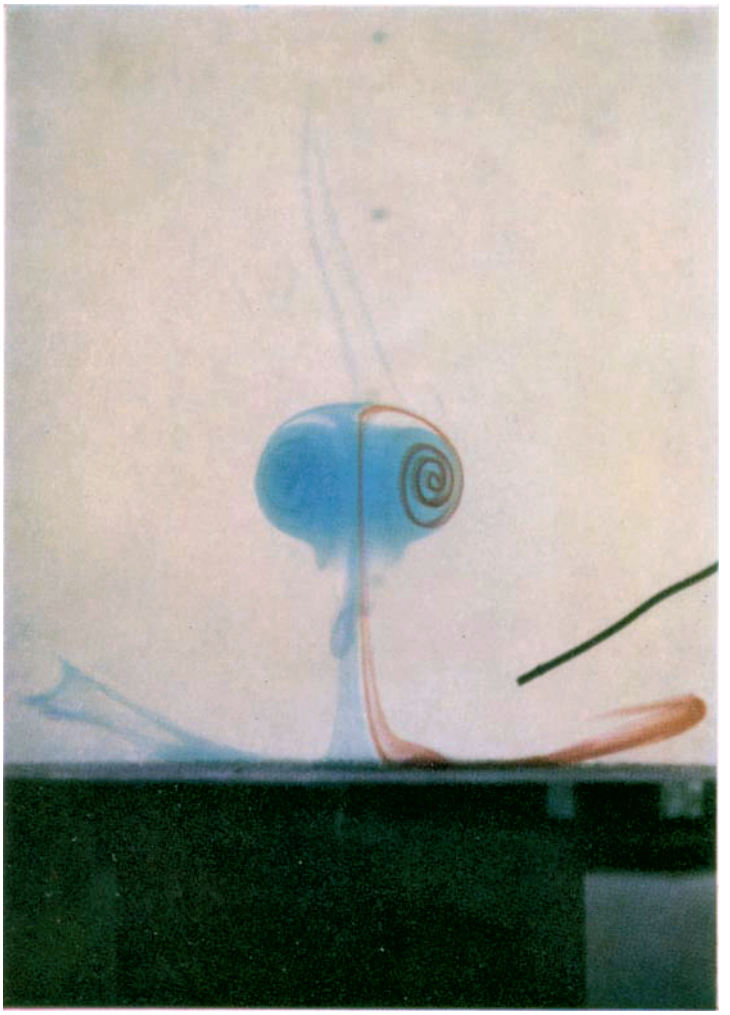

FIGURE 12. Photograph of the formation process shown in figure 11. Blue dye came from inside the chamber and the red fluid from the region close to the outside wall of the chamber.